HHS Public Access

Author manuscript

Ann Biomed Eng. Author manuscript; available in PMC 2021 June 01.

Published in final edited form as:

Ann Biomed Eng. 2020 June ; 48(6): 1850–1862. doi:10.1007/s10439-020-02497-x.

Targeting Cell Contractile Forces: A Novel Minimally Invasive Treatment Strategy for Fibrosis

Keerthi Atluri, **Sathivel Chinnathambi**, **Alyssa Mendenhall**, **James A. Martin**, **Edward A. Sander**, **Aliasger K. Salem**

University of Iowa, Iowa City, Iowa, 52242, USA

Abstract

Fibrosis is a complication of tendon injury where excessive scar tissue accumulates in and around the injured tissue, leading to painful and restricted joint motion. Unfortunately, fibrosis tends to recur after surgery, creating a need for alternative approaches to disrupt scar tissue. We posited a strategy founded on mechanobiological principles that collagen under tension generated by fibroblasts are resistant to degradation by collagenases. In this study, we tested the hypothesis that blebbistatin, a drug that inhibits cellular contractile forces, would increase the susceptibility of scar tissue to collagenase degradation.

Decellularized tendon scaffolds (DTS) were treated with bacterial collagenase with or without external or cell-mediated internal tension. External tension producing strains of 2–4% significantly reduced collagen degradation compared with non-tensioned controls. Internal tension exerted by human fibroblasts seeded on DTS significantly reduced the area of the scaffolds compared to acellular controls and inhibited collagen degradation compared to free-floating DTS. Treatment of cell-seeded DTS with 50 mM blebbistatin restored susceptibility to collagenase degradation, which was significantly greater than in untreated controls ($p < 0.01$). These findings suggest that therapies combining collagenases with drugs that reduce cell force generation should be considered in cases of tendon fibrosis that do not respond to physiotherapy.

KEY TERMS:

Blebbistatin; tendon; collagen; Decellularized Scaffolds; extracellular matrix; collagenases; matrix metalloproteinases; fibroblasts; mechanobiology; contracture

INTRODUCTION

Tendon fibrosis results from an aberrant wound healing response to tissue injury that is characterized by excessive collagen synthesis and contracture.21 Fibrotic tendons can be successfully treated by physical therapy, but surgical interventions are often required to fully

aliasger-salem@uiowa.edu.

restore range of motion. For example, in Dupuytren's contracture, a fibroproliferative condition of the palmar fascia, collagen is formed into dense contractile cords.4 Treatment involves removing or disrupting the cords via the manipulation of a needle inserted through the skin.16 Unfortunately, fibrosis tends to recur after this procedure, creating a need for non-surgical options. One solution that is being explored is to degrade extracellular matrix proteins, such as the collagens, using matrix metalloproteinases (MMPs). The U.S. Food and Drug Administration (FDA) has approved the administration of *Clostridium histolyticum* collagenase (CHC) for physiological cleavage of collagen to soften and weaken the fibrils in Dupuytren's contracture.32 Exogenous injection of collagenase is also being investigated for its potential to treat other fibrotic diseases, such as oral submucous fibrosis19, capsular fibrosis following silicone implantation, and urethral fibrosis.29 However, repeated injections of collagenase are required, which can lead to several complications including flexor tendon rupture, upper limb pain, edema, bruising, and skin perforation.7,25,30,33,36

Another factor that might reduce the effectiveness of collagenase is the local mechanical environment. Several studies indicate that stretched collagen can be strain-protected from degradation by collagenases.3,6,9,11,24,39 This strain can originate externally from surrounding tissue forces that are transmitted to the fibrotic tissue, or internally from cell traction forces applied to collagen fibers by resident cells, such as myofibroblasts. By attaching and pulling on the extracellular matrix (ECM), cells can actively sense changes in ECM rigidity, which in turn influences cell spreading, migration, proliferation, gene expression, and differentiation.20,34 Cells can also change the local ECM stiffness by pulling on local matrix fibers and removing "slack" in the matrix. These traction forces, usually in the nanoNewton (nN) range, are produced via actin-myosin engagement within the cytoskeleton and transmitted to ECM via focal adhesion complexes.15 As such, we hypothesize that elevated cell traction forces can protect collagen fibers from protease degradation. As a corollary, the effectiveness of collagenase injections can be significantly improved by simultaneously injecting biomolecules that can inhibit/reduce cell traction force generation. Thus, biomolecule-based force inhibition/reduction should allow collagen fibers to relax and become susceptible to enzymatic degradation.

One target for reducing traction force generation is the actin-myosin force generating apparatus of the cytoskeleton. The small, cell permeable molecule blebbistatin reversibly inhibits non-muscle myosin II (NMII) engagement with actin in a dose dependent manner, inhibiting internal force generation.18 Blebbistatin prevents the myosin head from releasing ADP, a critical step required to continue the power cycle that causes force generation.13

To test the hypothesis that cell contractile forces can inhibit the activity of CHC, we conducted a series of *in vitro* studies in which we measured the degradation rate of decellularized tendon scaffolds (DTS) re-cellularized with human fibroblasts immortalized by TERT transduction. We used DTS because it is largely composed of collagen and the collagen fibers are relatively aligned, which makes it easier to ensure that stretching the DTS along one direction means that a high percentage of collagen fibers are also stretched in that direction.

MATERIALS & METHODS

Decellularized Tendon Scaffolds (DTS)

Unused rabbit patellar tendons from a companion study1 were harvested and subjected to two freeze thaw cycles in 1X phosphate buffered saline (PBS) and 1% (v/v) penicillin, streptavidin, amphotericin (PSA) with 3 h of freezing at −80 °C followed by 3 h of thawing at room temperature. The tendons were then decellularized using 500 mL of 0.5% (w/v) sodium dodecyl sulfate (SDS), 0.5% (v/v) Triton X-100, and 1% (v/v) PSA in 1X PBS adjusted to pH 7.4 for 3 to 4 days with a daily solution change. The tendons were then stored in 500 mL of ultrapure water adjusted to pH 7.4 using 1N NaOH for 7 to 10 days. The tendons were then frozen sectioned with a cryotome into 50 μm thick sections. The sections were then washed for 48 to 72 h in 100 mL of 1X PBS with a solution change every 12 h.5,10,35,37

The sections were then sterilized with 50 mL of 0.1% v/v peracetic acid and 10% v/v PSA in 1X PBS for 24 h and then rinsed twice over 24 h in 100 mL of serum free DMEM, or until no changes in DMEM color was observed. Each section, referred to as a DTS, was cut to a uniform size (~ 1 cm × 0.5 cm) and the wet weight was recorded. Each DTS was imaged to ensure that no visible defects were present. The extent of decellularization was also estimated by staining the sections before and after decellularization using ethidium bromide (528/617 nm) (LIVE/DEAD™ Viability/Cytotoxicity Kit, for mammalian cells; ThermoFisher Scientific; L3224) for dead cells. (Fig. 1)

Stretching Device

DTS were subjected to uniaxial tensile stretch using a custom-built device (Fig. 1). The stretching device consisted of a two-piece stage with one fixed and one movable part. The pieces were connected with a stainless-steel rod that allowed adjustable, uniaxial translation via the adjustment of a connected, overhead screw. Before use, the devices were submerged overnight in 70% ethanol and exposed to UV light for at least 2 h on each side. Two grips clamped each end of the DTS to the stage using stainless steel miniature screws. The distance between the grips, and thus the tension applied to the DTS, was controlled by adjusting the miniature screw gauge.

To ensure that similar stretch/tension was exerted on all the samples, digital images of each DTS were taken before and after their placement on the stretching device and before fixing the grips. The lengths of the DTS were measured using ImageJ software. The lengths of the DTS present on the stage were subtracted from the initial length of the DTS to determine the actual DTS length that was subjected to stretch. Furthermore, DTS were stretched until there was no sag and this point was considered as the baseline. Using micrometer screw gauge, the amount of stretch applied was controlled.

Calibration Curve for DTS Degradation Assessment

Several wet DTS obtained from different rabbit patellar tendons were pooled together and cut into pieces ~2 mm × 2 mm. Wet weights ranging from 0.5 mg to 15 mg were analyzed for hydroxyproline content to obtain a calibration curve. Hydroxyproline assay was

performed as described below. The percent degradation of collagen was then calculated using the calibration curve to transform wet weight vs collagen content (data not shown).

DTS Degradation Assessment

Pre-weighed DTS were immersed in 5 mL of phenol red free and serum free DMEM containing 0.3 mg/mL collagenase and 5 mM $CaCl_2$ and subjected to either 0, 2, 4, or 8% engineering strain. DTS were maintained in an incubator at 37 °C with 5%/95% CO_2/air. After respective time points supernatant medium samples were collected for hydroxyproline assay for collagen degradation assessment of DTS (Fig. 2) and the remnants of treated DTS samples were subjected to scanning electron microscopic imaging (SEM) (Fig. 3). The collagenase concentration to be used was determined based on the previous experiments in which a wide range of collagenase concentrations ranging from 0.05 mg/mL to 2 mg/mL were assessed. The minimum concentration at which DTS got completely degraded was selected.

Medium samples of 5 mL volume were collected at 1, 3, 5, 7, 24 and 48 h (Fig. 2) and were dried using rotary vapor evaporator and analyzed for collagen content using a hydroxyproline assay as described in detail previously.2 Briefly, phenol red free DMEM was used to prevent any interference with colorimetric hydroxyproline detection. The remnants of supernatant samples after collagenase treatment were hydrolyzed in 0.1M NaOH at 98°C for one hour. Samples were centrifuged, the supernatant containing collagen was separated from the pellet containing elastin and was dried, then hydrolyzed in 6N HCl at 110°C for 2 h, and finally re-dried in a speed vacuum for 1.5 h. Absorbance of the standard and samples were measured at 570 nm with a microplate reader (Glomax, Multi-detection system, Promega, Madison, WI). The amount of hydroxyproline was measured as an estimation of the amount of collagen in response to treatment by assuming 1 μg of 4-hydroxyproline per 7.46 μg of collagen.8,28 Statistical analysis was performed using a one-way ANOVA and Tukey post hoc test with n=6.

Recellularized Tendon Scaffolds (RTS)

Pre-weighed DTS were transferred into individual glass vials and then sterilized using 0.1% v/v peracetic acid and 1% (v/v) PSA in 1X PBS and sterilized for 24 h. DTS were then transferred to serum free DMEM with 1% PSA that was replaced twice over 24 h. DTS were incubated in 100% FBS for 1 h and then transferred to 100 mm petri plates and allowed to dry for 10 min. DTS were seeded with 5 million human telomerase reverse transcriptase (TERT) fibroblasts suspended in 80 μL DMEM with 10% FBS. The suspension was added in 20 μL increments, twice on each side with a 30-minute gap between each addition, to ensure complete cell coverage of the scaffold. Control tendon scaffolds (CTS) were treated in the same manner using DMEM with 10% FBS but no cells. After 30 min, the RTS were rinsed twice with DMEM to remove unattached cells and then incubated in serum containing DMEM. RTS were then incubated for 6 h to ensure cell attachment. After 6 h, cell viability was assessed with live/dead stain and with 3 μg/mL Hoechst 3,33,4,2. RTS were imaged using a confocal microscope (Olympus FLUOVIEW FV1000, PA, USA) (Fig. 4A) and SEM (Fig. 4B). RTS and CTS were immersed in serum-free DMEM with 5 mM Ca^{2+} ($CaCl_2$) and 0.3 mg/mL collagenase to assess susceptibility to degradation.

RTS Cell Number

RTS cell number was assessed with an MTS assay (n=3) (Fig. 4C). Cell concentrations ranging from 5,000 to 100,000 cells per well were seeded in a 24 well plate for 24 h to obtain a standard curve. After 24 h, RTS were placed into the wells of 24 well plate containing fresh 500 μL of DMEM with 10% FBS. 100 μL of MTS assay reagent (3-(4,5-dimethylthiazol-2-yl)-5-(3-carboxymethoxyphenyl)-2-(4-sulfophenyl)-2H-tetrazolium) was added to each well. The plates were then incubated for 2 h at 37 °C and 5% CO_2. After 2 h, 120 μL of the solution from each well was transferred to the wells of a 96 well plate and the cell viability was determined by assessing the relative levels of soluble formazan formed using a SpectraMax Plus384 (Molecular Devices, Sunnyvale, CA, USA) microplate reader at an absorbance of 490 nm. Statistical analysis was performed using unpaired two tailed t-test with n = 3.

RTS Area Measurements

A decrease in RTS area is an indicator of fibroblast force generation. RTS were treated with 50 μM blebbistatin in dimethyl sulfoxide (DMSO) was considered as a treatment group and the RTS without blebbistatin treatment and treated with 0.5% (v/v) DMSO was considered as a control group. DTS were seeded with cells as described previously and imaged at 0 h and 24 h. Images were analyzed in ImageJ (NIH, Bethesda, MD) using the wand tracing tool to select and measure DTS area at each time point (Fig. 5). Statistical analysis was performed using a one-way ANOVA and Tukey post hoc test with n=3. The amount of blebbistatin used (50 μM) was based on our previous study in which various concentrations of blebbistatin ranging from 5 μM to 200 μM was assessed on cell viability using MTS assay. Based on the cell viability data, we have chosen 50 μM as the maximum concentration, as it didn’t affect the cell viability significantly.

RTS Force Measurements

Contractile force measurements generated in the RTS were measured by monitoring the amount of deflection in a calibrated Nitinol (NiTi) wire. Wire deflections were converted to force with the wire calibration curve (Fig. 6A–B). The NiTi wire system consisted of a stretching device mounted to a 100 mm × 20 mm tissue culture dish (Fig. 6C–D). A rigid capillary tube of 1 mm diameter was attached to the stationary end and a 60 mm long NiTi wire (0.0075-inch diameter; Confluent P/N – WSE000750000SG) was attached to the adjustable end of the device. RTS were attached both the tube and the wire. The device was then adjusted to remove RTS slack. In order to allow isometric tension to develop, a 0.5 mm diameter stainless-steel needle was place through the end of capillary tube. A groove at the end of the needle held the NiTi wire in place and prevented it from deflecting. After 24 h, the needle was removed carefully using forceps. Images were acquired before and after removing the needle in order to measure the force generated within the RTS. To confirm that the displacement of the wire was solely due to contractile forces from the cells, DTS were placed in the system as a control.

RTS Collagen Degradation

Six hours after cell seeding, RTS were mechanically constrained in the stretching devices and the cells were allowed to exert contractile forces for 24 h. The RTS were elongated to remove sag by adjusting the distance between grips in the stretching device in order to allow the cells to generate isometric tension in the scaffold. In parallel, 50 μM blebbistatin in 0.5% (v/v) DMSO was added immediately after securing the RTS to the stretching devices. Free floating RTS, free floating RTS treated with blebbistatin, and mechanically constrained RTS without blebbistatin served as controls. After 24 h, the RTSs were treated with serum-free and phenol red free DMEM containing 0.3 mg/mL collagenase/5 mM Ca^{++} ($CaCl_2$) for 1, 3, 5, 7, and 24 h. Medium was collected and processed as described above. After drying, sample remnants were subjected to a hydroxyproline assay as described above (Fig. 7). Statistical analysis was performed using a one-way ANOVA and Tukey post hoc test with n=6.

Scanning Electron Microscopic (SEM) Imaging

DTS and RTS were fixed with 4% paraformaldehyde in 0.1 M sodium cacodylate for 1 h followed by 2% (v/v) osmium tetroxide in 0.1 M sodium cacodylate treatment for 30 minutes. The sections were then subjected to sequential dehydration using percentages of ethanol ranging from 25% to 100% (v/v) for 4 minutes each. DTS were treated with hexamethyldisilazane (HMDS) for 10 min before mounting the sections on aluminum stubs with carbon tape. The sections on the stubs were sputter coated with a 5 nm thick layer of gold–palladium by an argon beam K550 sputter coater (Emitech Ltd., Kent, England) and imaged with a Hitachi S-4800 Field-Emission SEM (Hitachi Ltd., Tokyo, Japan). Images were captured at 4 kV accelerating voltage under an argon atmosphere.

Statistical Analysis

Statistical analysis was performed using either one-way ANOVA followed by Tukey post hoc test or unpaired t-test with GraphPad PRISM (GraphPad, San Diego CA). Data are expressed as mean ± standard deviation (*$p<0.05$; **$p<0.01$; ***$p<0.001$).

RESULTS

DTS

DTS were stained with EtBr and CNA35 in order to visualize dead cells and collagen, respectively. Confocal images revealed that prior to decellularization, dead cells were abundant in DTS (Fig. 1D). After decellularization, no sign of cells remained (Fig. 1E), confirming that the decellularization process was successful. To assess whether the decellularization process grossly impacted DTS fiber structure, DTS were imaged via SEM. Fibril diameters appeared unaffected by decellularization and remained highly aligned (Fig. 1F, G). Therefore, it can be concluded that the decellularization process did not appreciably alter collagen fiber alignment.

Effect of external tension on the degradation rate of DTS

DTS were subjected to strains ranging from 0% to 8% as described earlier. After 24 h of collagenase treatment, DTS subjected to 8% strain had degraded 75.3% ± 12.5% (Fig. 2A), significantly more so than DTS subjected to 2% strain (23.7±19.8%, **$p<0.01$) and 4% (35.1% ± 33.8%, *$p<0.05$). Though not significant the degradation of DTS at 8% strain was higher than DTS subjected to 0% strain (68.5% ± 14.8%) and free-floating DTS (61.1% ± 24.3%).

DTS degradation rates in the presence of collagenase (Fig. 2B) were lowest for strains of 2% (0.76%/h) and 4% (0.87%/h). At 8% strain the degradation rate (1.8%/h) greatly increased; it was even higher than the rate for free floating DTS (1.35%/h) and DTS under 0% strain (1.59%/h).

SEM images (Fig. 3) also demonstrate that there was no significant impact on DTS fibril diameter, fibril microstructure, and fibril orientation under 2% and 4% strain after 7 h of collagenase treatment compared to the untreated DTS. In contrast, fibril diameter decreased, and fibril orientation was disrupted in free floating, 0%, and 8% strain. These data indicate that DTS subjected to between 2% and 4% strain do not degrade as quickly in the presence of collagenase. Statistical analysis was performed using a one-way ANOVA and Tukey post hoc test with n=6.

RTS

Approximately 10% of the cells added to the DTS attached (Fig. 4). Confocal and SEM images revealed that the cells attached to the RTS aligned and oriented along the axes of the fibrils (Fig. 5 A, B left). Blebbistatin treated cells remained attached but became more rounded in morphology (Fig. 5 A, B right). No significant differences in cell number per unit area (~30,000 cells/cm^2) were observed between RTS treated with or without blebbistatin (Fig. 5C), which indicates that blebbistatin did not affect cell viability and proliferation over the duration of the experiment. Statistical analysis was performed using unpaired two tailed t-test with n = 3.

As we know that cells exert contractile forces and pull the matrix, a reduction in RTS area was used as an indicator of cell force generation.1,2 After 24 h, RTS experienced a reduction in area of approximately 30%. Addition of 50 μM blebbistatin in DMSO prevented a reduction in RTS area and did not differ significantly from the DTS controls (Fig. 5). Statistical analysis was performed using a one-way ANOVA and Tukey post hoc test with n=3. Direct cell force measurements with the NiTi wire system (Fig. 6) were found to be 72 nN after 24 h. No wire deflection was observed in control DTS.

Effect of cell traction forces on the degradation rate of RTS

To determine whether cell contractile forces can protect RTS from degradation by collagenases, RTS that had been allowed to generate isometric tension while secured in the stretching device for 24 h (i.e., fixed-boundary RTS) were treated with collagenase. Degradation rates were compared with unconstrained, free-floating RTS that were either treated or untreated with blebbistatin.

Degradation rate profiling showed that fixed-boundary RTS degraded at a much lower rate (1.6%/h) than any other group (Fig. 7). Treatment of fixed boundary RTS with blebbistatin resulted in a degradation rate of 2.7%/h, which was comparable to free-floating DTS cultures with or without blebbistatin treatment (2.8%/h and 2.4%/h respectively).

Free floating RTS treated or untreated with blebbistatin degraded to greater extent, 68.7% ±14.7% (**$p<0.01$) and 57.7% ± 10.6%, respectively, compared to the RTS with fixed boundaries (39.2% ± 8.9%) (Fig. 7). Fixed-boundary RTS treated with blebbistatin degraded more (*$p<0.05$) than untreated fixed-boundary RTS, and they degraded similarly to untreated free-floating RTS, indicating that cell tractions reduced collagenase activity in a manner similar to the effect of applying 2%–4% strain on DTS. SEM images (Fig. 8) revealed that fixed-boundary RTS degraded less and retained more fibril organization in the presence of collagenase than for the other conditions tested. Statistical analysis was performed using a one-way ANOVA and Tukey post hoc test with n=6.

DISCUSSION

Fibrosis is a condition where excess collagen accumulates, and it is associated with an impaired degradative environment.22 The triple helix is highly resistant to proteolysis and thus collagen degradation requires a specialized class of proteases called matrix metalloproteinases. Most of the research was based on the regulation of biochemical pathways such as MMP/TIMP balance, myofibroblast phenotypic conversion by TGF-β etc. on the rate of collagen synthesis and degradation. A few studies have indicated the influence of matrix mechanical properties on the phenotypic behavior of fibroblasts, effect of external load on collagen protection and their implications on fibrosis. However, no work has been done to account for the importance of mechanical strain exerted by cell contractile forces in inhibiting collagen degradation by MMPs in tissue fibrosis.

MMP activity is regulated by mechanical stress on fibrillary collagen that inhibits proteolysis through an unknown mechanism. Conformational change in triple helix is necessary for inhibition. Intermolecular triple helical forces as the macromolecular forces are transferred to α-chains of triple helix through intermolecular kinks and the cross links between triple helices produces conformational change. This study highlights the importance of cell contractile forces in stabilizing collagen from collagenase induced enzymatic degradation.

Thus, in this study, we hypothesize that the cell contractile forces can protect collagen fibers from enzymatic degradation and the effectiveness of enzymatic treatment can be significantly improved by treating cells with biomolecules that are capable of inhibiting/reducing cell traction force generation such as blebbistatin.

Before showing the effect of mechanical forces exerted by cell contractile action, we demonstrated the influence of external strain on collagen protection action on DTS. Previous studies have shown that the external strain could protect collagen from collagenase induced degradation. For example, Flynn et al showed that the degradation time of reconstituted type I collagen micronetworks subjected to mechanical strain were significantly enhanced

compared to the unstrained collagen fibrils in the presence of active matrix metalloproteinase 8 (MMP-8).9 Sato et al, demonstrated that when lung tissue strips were subjected to a 20% strain, the tissue strips were protected against collagenase induced degradation compared to the strips at higher and lower strains.38 Huang et al., showed that a strain level of 4% was enough to protect insoluble collagen fibers where a minimum degradation was observed.14 Our results show that the external strains of 2% and 4% can protect ECM from degradation up to 48 h and only about 30% degradation was noticed at the end of 48 h, which agrees with previous studies.

However, at 8% strain the degradation was significantly higher compared to the 2% and 4% strains and was higher even when compared to the free floating or 0% strain DTS. This result can probably be explained by the breakage of collagen fibrils resulting in the exposure of more enzymatic cleavage sites to collagenase activity. The study done by Rigby et al. explained this phenomenon well. They showed that the tendon became progressively weaker with each extension at strains beyond 4% suggesting the rupturing of secondary bonds adjoining the adjacent molecular units. The extension involves unwinding of loops or folds during which the secondary bonds are irreversibly broken resulting in the permanent separation of groups on the amino acid residues responsible for the bond.26 The enhanced degradation of DTS at 8% external strain may have been due to covalent linkage fracture of the collagen molecular chains and slippages between the unit molecular chains.17 The exposed fibrils might have made it easier for collagenase to access the binding sites resulting in enhanced degradation of the matrix even when compared to the unstretched and free-floating matrices.

Orientation, realignment and synthesis of collagen fibers in the ECM is dictated by cellular orientation and contractile force exertion.12,23,31 The exertion of cell contractile forces on DTS in this study was confirmed by decrease in area and NiTi wire displacement. Results from NiTi wire displacement showed that approximately 70 pN of force was exerted by the cells present on RTS. As there were approximately 30,000 cells per RTS, the average force per cell can be estimated at 2.4 pN. Jansen *et al.* demonstrated that human CCL-224 fibroblasts by exerting an average force between 2 and 10 pN on each fibrin fiber depending on the cell density and fibrin concentration can produce stiffening equivalent to an external stress of 14 Pa. by shearing actin networks. From this we can assume that the cells by exerting 70 pN of force (as measured by NiTi wire displacement) will be able to induce active stiffening of matrices.15

Matrix degradation by collagenase was a related factor affecting tension. The least degradation was in cell-seeded DTS under external tension, whilst the most degradation was in acellular DTS in the absence of external tension. Blebbistatin treatment increased degradation in cell-seeded DTS, confirming that cellular contractile forces can play a role in collagenase vulnerability. Though not significant, the DTS with cells and fixed boundaries were shown to have less degradation compared to free floating DTS with cells. When this cell generated strain on DTS with fixed boundaries is compared to the external strain, the DTS with cell generated strain have shown to produce the same effect on collagen stabilization as with the 2% external strain where the degradation was only about approx. 30% after 24 h of collagenase treatment. Thus, it can be concluded that 70 pN of force was

sufficient to provide resistance to collagen degradation and is comparable to 2% externally exerted strain. These results agree with other studies. For example, a study by Chang et al, demonstrated that approximately 100 pN of applied force on heterotrimer collagen chains can stabilize the cleavage sites resulting in force induced stabilization. However, a small force of 10 pN can be enough to stabilize the system.6 Ruberti et al. showed that when 15–30 pN of force was applied on individual type I/V collagen monomers will not only reduce the configurational entropy of monomers in the fibril but is also capable of producing axial deformation of monomers making enzyme binding and cleavage more difficult.27

From the above data we can conclude that because cellular contractile forces can significantly inhibit the degradative activity of collagenases, blebbistatin may enhance the effectiveness of collagenase-based therapies for Dupuytren's contracture and other forms of fibrosis.

ACKNOWLEDGEMENTS

This study was sponsored by The Department of Defense (award # W81XWH-14-1-0327), National Institutes of Health (P30 CA086862) and the Lyle and Sharon Bighley Chair of Pharmaceutical Sciences.

ABBREVIATIONS

DTS	Decellularized Tendon Scaffolds
MMPs	Matrix Metalloproteinases
FDA	U.S. Food and Drug Administration
CHC	*Clostridium Histolyticum* Collagenase
Nn	Nanonewton
NMII	Non-Muscle Myosin II
DTS	Decellularized Tendon Scaffolds
PBS	Phosphate Buffered Saline
PSA	Penicillin, Streptavidin, Amphotericin
SDS	Sodium Dodecyl Sulfate
RTS	Recellularized Tendon Scaffolds
TERT	Telomerase Reverse Transcriptase
DMSO	Dimethyl Sulfoxide
CTS	Control Tendon Scaffolds
Niti	Nitinol
SEM	Scanning Electron Microscopic

HMDS	Hexamethyldisilazane
MMP-8	Matrix Metalloproteinase 8

REFERENCES

1. Atluri K, Brouillette MJ, Seol D, Khorsand B, Sander E, Salem AK, Fredericks D, Petersen E, Smith S, Fowler TP, and Martin JA. Sulfasalazine Resolves Joint Stiffness in a Rabbit Model of Arthrofibrosis. JOR Spine. 2019.
2. Atluri K, De Jesus AM, Chinnathambi S, Brouillette MJ, Martin JA, Salem AK and Sander EA. Blebbistatin-Loaded Poly(d,l-lactide-co-glycolide) Particles For Treating Arthrofibrosis. ACS Biomater Sci Eng. 2:1097–1107, 2016.
3. Bhole AP, Flynn BP, Liles M, Saeidi N, Dimarzio CA, and Ruberti JW. Mechanical strain enhances survivability of collagen micronetworks in the presence of collagenase: implications for load-bearing matrix growth and stability. Philos Trans A Math Phys Eng Sci. 367:3339–3362, 2009. [PubMed: 19657003]
4. Brandes G, Messina A, Reale E. The palmar fascia after treatment by the continuous extension technique for Dupuytren's contracture. J Hand Surg Eur Vol. 19:528–533, 1994.
5. Burk J, Ruberti I, Berner D, Kacza J, Kasper C, and Pfeiffer B. Freeze-thaw cycles enhance decellularization of large tendons. Tissue Eng Part C Methods. 20:276–284, 2014. [PubMed: 23879725]
6. Chang SW, Flynn BP, Ruberti JW, and Buehler MJ. Molecular mechanism of force induced stabilization of collagen against enzymatic breakdown. Biomaterials. 33:3852–3859, 2012. [PubMed: 22401852]
7. Denkler KA, Vaughn CJ, Dolan EL, and Hansen SL. Evidence-Based Medicine: Options for Dupuytren's Contracture: Incise, Excise, and Dissolve. Plast Reconstr Surg. 139:240e–255e, 2017.
8. Dombi GW, Haut RC, and Sullivan WG. Correlation of high-speed tensile strength with collagen content in control and lathyritic rat skin. 54:21–28, 1993.
9. Flynn BP, Bhole AP, Saeidi N, Liles M, Dimarzio CA, and Ruberti JW. Mechanical strain stabilizes reconstituted collagen fibrils against enzymatic degradation by mammalian collagenase matrix metalloproteinase 8 (MMP-8). PLoS One. 5: e12337, 2010. [PubMed: 20808784]
10. Gilbert TW, Sellaro TL, and Badylak SF. Decellularization of tissues and organs. Biomaterials. 27:3675–3683, 2006. [PubMed: 16519932]
11. Gyoneva L, Hovell CB, Pewowaruk RJ, Dorfman KD, Segal Y, and Barocas VH. Cell-matrix interaction during strain-dependent remodelling of simulated collagen networks. Interface Focus. 6:20150069, 2016. [PubMed: 26855754]
12. Harris AK, Stopak D, and Wild P. Fibroblast traction as a mechanism for collagen morphogenesis. Nature. 290:249–251, 1981. [PubMed: 7207616]
13. Houdusse A, and Sweeney HL. How Myosin Generates Force on Actin Filaments. Trends Biochem Sci. 41:989–997, 2016. [PubMed: 27717739]
14. Huang C, and Yannas IV. Mechanochemical studies of enzymatic degradation of insoluble collagen fibers. J Biomed Mater Res. 11:137–154, 1977. [PubMed: 14968]
15. Jansen KA, Bacabac RG, Piechocka IK, and Koenderink GH. Cells actively stiffen fibrin networks by generating contractile stress. Biophys J. 105:2240–2251, 2013 [PubMed: 24268136]
16. Ketchum LD, The Rationale for Treating the Nodule in Dupuytren's Disease. Plast Reconstr Surg Glob Open. 2:e278, 2014. [PubMed: 25587512]
17. Komatsu K, Mechanical strength and viscoelastic response of the periodontal ligament in relation to structure. J Dent Biomech. 2010: 502318, 2010. [PubMed: 20948569]
18. Kovacs M, Toth J, Hetenyi C, Malnasi-Csizmadia A, and Sellers JR. Mechanism of blebbistatin inhibition of myosin II. J Biol Chem. 279:35557–35563, 2004. [PubMed: 15205456]
19. Lin HJ, and Lin JC. Treatment of oral submucous fibrosis by collagenase: effects on oral opening and eating function. Oral Dis. 13:407–413, 2007. [PubMed: 17577328]

20. Liu AP, Chaudhuri O, and Parekh SH. New advances in probing cell-extracellular matrix interactions. Integr Biol (Camb). 9:383–405, 2017. [PubMed: 28352896]
21. Mann CJ, Perdiguero E, Kharraz Y, Aguilar S, Pessina P, and Serrano AL. Aberrant repair and fibrosis development in skeletal muscle. Skelet Muscle. 1:21, 2011. [PubMed: 21798099]
22. McKleroy W, Lee TH, and Atabai K. Always cleave up your mess: targeting collagen degradation to treat tissue fibrosis. Am J Physiol Lung Cell Mol Physiol. 304:L709–721, 2013. [PubMed: 23564511]
23. Meshel AS, Wei Q, Adelstein RS, and Sheetz MP. Basic mechanism of three-dimensional collagen fibre transport by fibroblasts. Nat Cell Biol. 7:157–164, 2005. [PubMed: 15654332]
24. Nabeshima Y, Grood ES, Sakurai A, and Herman JH. Uniaxial tension inhibits tendon collagen degradation by collagenase in vitro. J Orthop Res. 14:123–130, 1996. [PubMed: 8618154]
25. Namazi H, and Majd Z. Cold intolerance following collagenase Clostridium histolyticum treatment for Dupuytren contracture: a molecular mechanism. J Hand Surg Am. 39:1886–1887, 2014. [PubMed: 25154579]
26. Rigby BJ, Hirai N, Spikes JD, and Eyring H. The Mechanical Properties of Rat Tail Tendon. J Gen Physiol. 43:265–283, 1959. [PubMed: 19873525]
27. Ruberti JW, and Hallab NJ. Strain-controlled enzymatic cleavage of collagen in loaded matrix. Biochem Biophys Res Commun. 336:483–489, 2005. [PubMed: 16140272]
28. Sander EA, Barocas VH, and Tranquillo RT. Initial fiber alignment pattern alters extracellular matrix synthesis in fibroblast-populated fibrin gel cruciforms and correlates with predicted tension. Ann Biomed Eng. 39:714–729, 2011. [PubMed: 21046467]
29. Sangkum P, Yafi FA, Kim H, Bouljihad M, Ranjan M, and Datta A. Collagenase Clostridium histolyticum (Xiaflex) for the Treatment of Urethral Stricture Disease in a Rat Model of Urethral Fibrosis. Urology. 86:647e1–647 e6, 2015. [PubMed: 26126692]
30. Sanjuan-Cervero R, Carrera-Hueso FJ, Vazquez-Ferreiro P, and Gomez-Herrero D. Adverse Effects of Collagenase in the Treatment of Dupuytren Disease: A Systematic Review. BioDrugs. 31:105–115, 2017. [PubMed: 28181175]
31. Stopak D, and Harris AK. Connective tissue morphogenesis by fibroblast traction. I. Tissue culture observations. Dev Biol. 90:383–398, 1982. [PubMed: 7075867]
32. Thomas A, and Bayat A. The emerging role of Clostridium histolyticum collagenase in the treatment of Dupuytren disease. Ther Clin Risk Manag. 6:557–572, 2010. [PubMed: 21127696]
33. Warwick D, Arandes-Renu JM, Pajardi G, Witthaut J, and Hurst LC. Collagenase Clostridium histolyticum: emerging practice patterns and treatment advances. J Plast Surg Hand Surg. 50:251–261, 2016. [PubMed: 27050718]
34. Wells RG, The role of matrix stiffness in regulating cell behavior. Hepatology. 47:1394–1400, 2008. [PubMed: 18307210]
35. Woon CY, Farnebo S, Schmitt T, Kraus A, Megerle K, and Pham H, et al. Human flexor tendon tissue engineering: revitalization of biostatic allograft scaffolds. Tissue Eng Part A. 18:2406–2417, 2012. [PubMed: 22712522]
36. Wozniczka J, Canepa C, Mirarchi A, and Solomon JS. Complications Following Collagenase Treatment for Dupuytren Contracture. Hand (N Y). 12:NP148–NP151, 2017. [PubMed: 28635316]
37. Xu H, Xu B, Yang Q, Li X, Ma X, and Xia Q, et al. Comparison of decellularization protocols for preparing a decellularized porcine annulus fibrosus scaffold. PLoS One. 9:e86723, 2014. [PubMed: 24475172]
38. Yi E, Sato S, Takahashi A, Parameswaran H, Blute TA, and Bartolak-Suki E. Mechanical Forces Accelerate Collagen Digestion by Bacterial Collagenase in Lung Tissue Strips. Front Physiol. 7:287, 2016. [PubMed: 27462275]
39. Zareian R, Church KP, Saeidi N, Flynn BP, Beale JW, and Ruberti JW. Probing collagen/enzyme mechanochemistry in native tissue with dynamic, enzyme-induced creep. Langmuir. 26:9917–9926, 2010. [PubMed: 20429513]

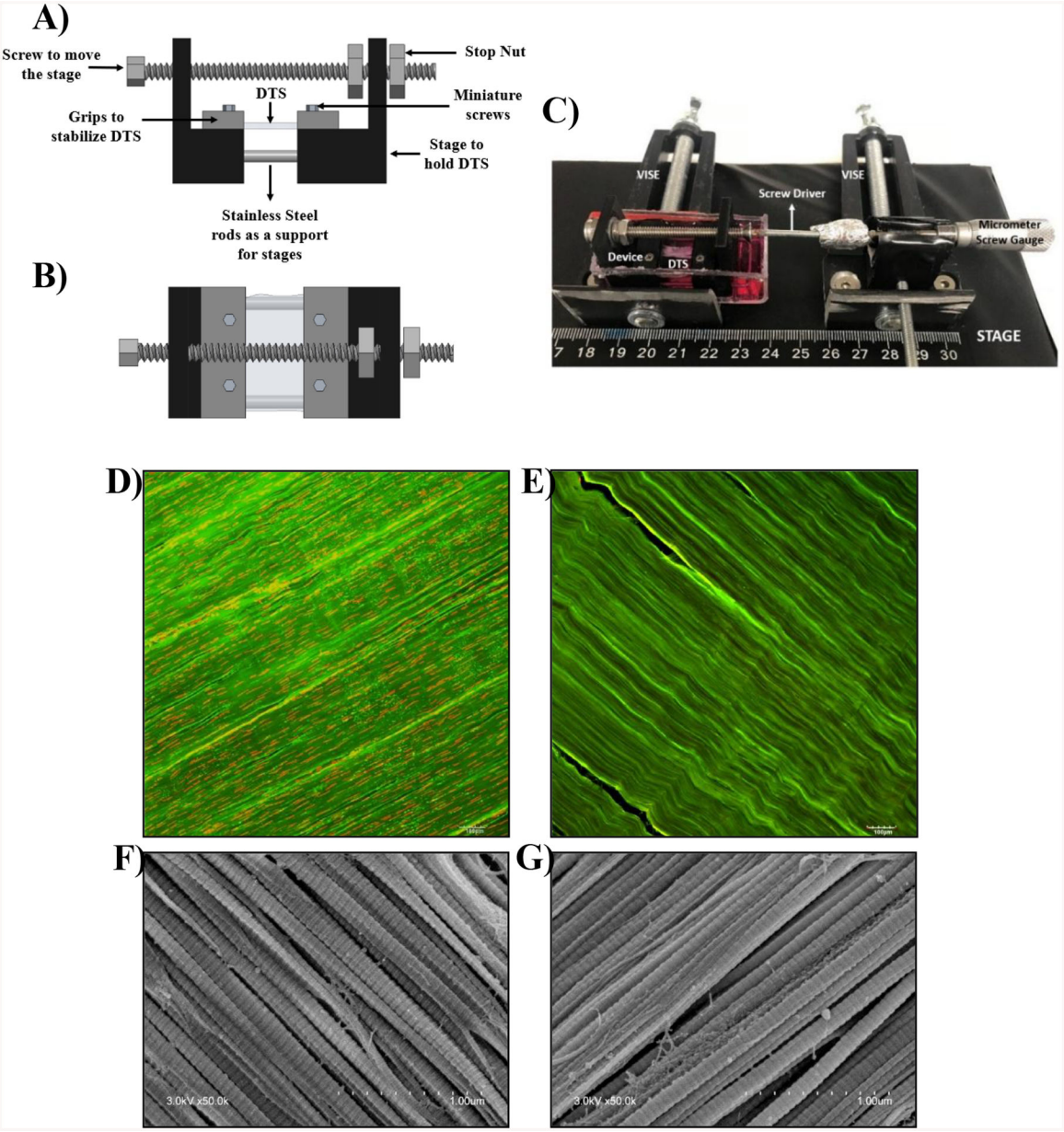

Figure 1:

Schematic of DTS stretching device: **A)** side view **B)** top view **C)** image showing the process of stretching DTS gripped in position on a stretching device using a micrometer screw gauge to achieve a certain displacement for accurate strain exertion. Confocal images of DTS stained with ethidium bromide (red) D**)** before decellularization and **E)** after decellularization. SEM images of DTS **F)** before decellularization and **G)** after decellularization

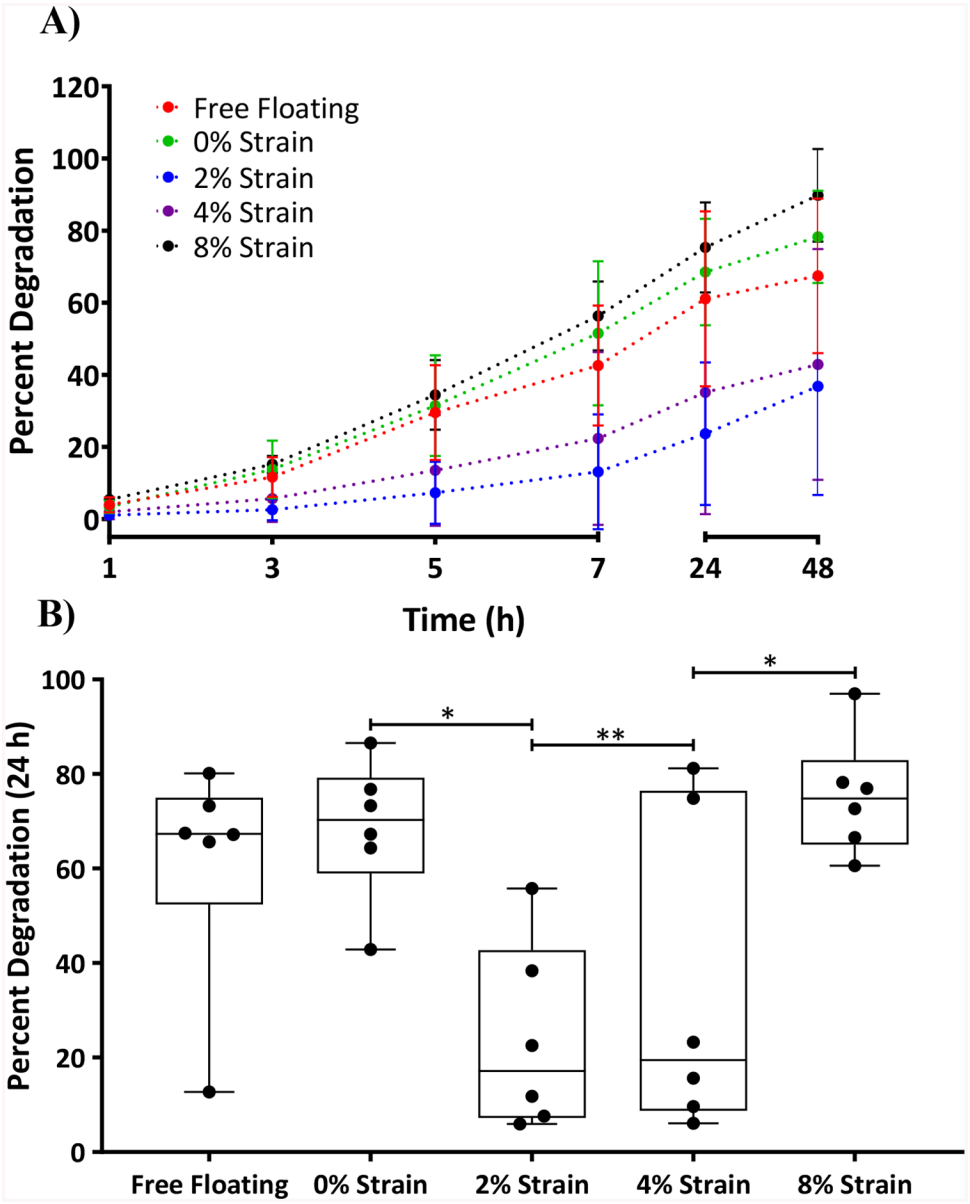

Figure 2:

Top – A) Graph showing percent degradation time profile of ECMs subjected to various strain conditions and at time points 1, 3, 5, 7, 24 and 48 h. **Bottom – B)** For the sake of clarity, the same 24 h data point as shown in Figure 2 A was represented in a bar graph showing percent degradation of DTS at various strains applied using a stretching device. Statistical analysis was performed using a one-way ANOVA and Tukey post hoc test with n=6. **p<0.05; **p<0.01.*

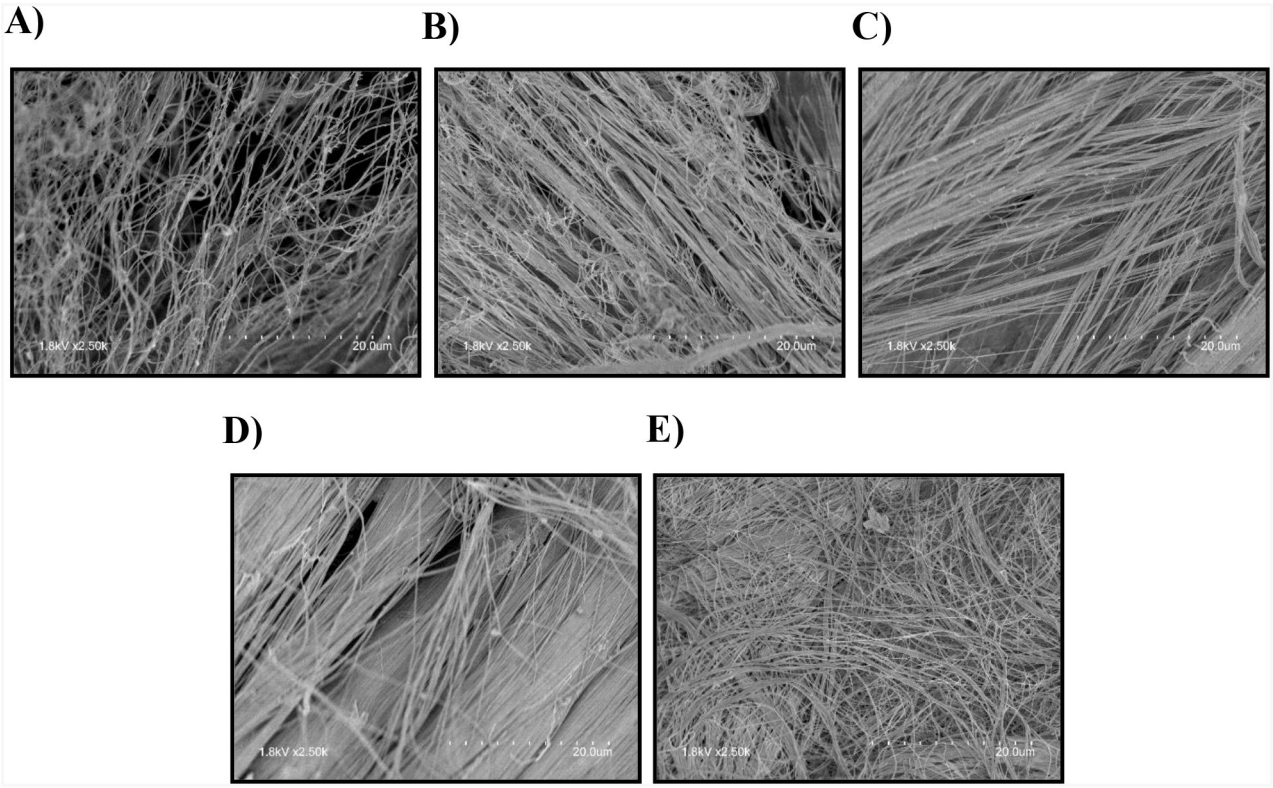

Figure 3:

Representative SEM images after 7 h of collagenase treatment **A)** Free floating DTS; **B)** DTS with 0% strain; **C)** DTS with 2% strain; **D)** DTS with 4% strain **E)** DTS with 8% strain

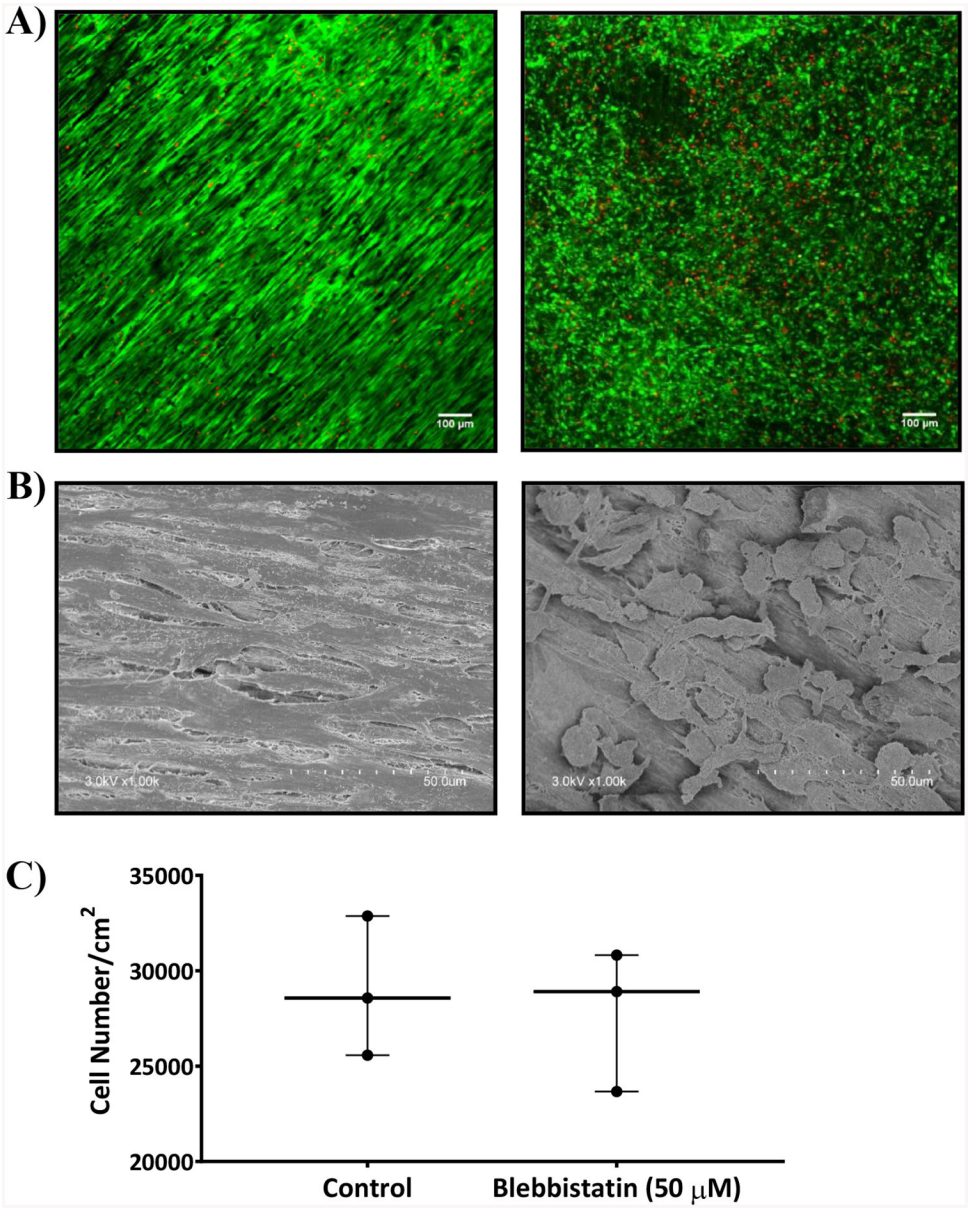

Figure 4:

A) Confocal images **B)** SEM images of untreated DTS seeded with human TERT fibroblasts (left) and 50 μM blebbistatin treated DTS (right) after 6 h of seeding cells. Both were stained with calcein AM (green) and ethidium bromide (red). The cells treated with blebbistatin changed morphologically from highly branched and spindle shaped (left) to rounded (right). **C)** Graph showing the cell number per cm^2 measured using MTS cell proliferation assay either treated or untreated with 50 μM blebbistatin. Statistical analysis was performed using unpaired two tailed t-test with n = 3.

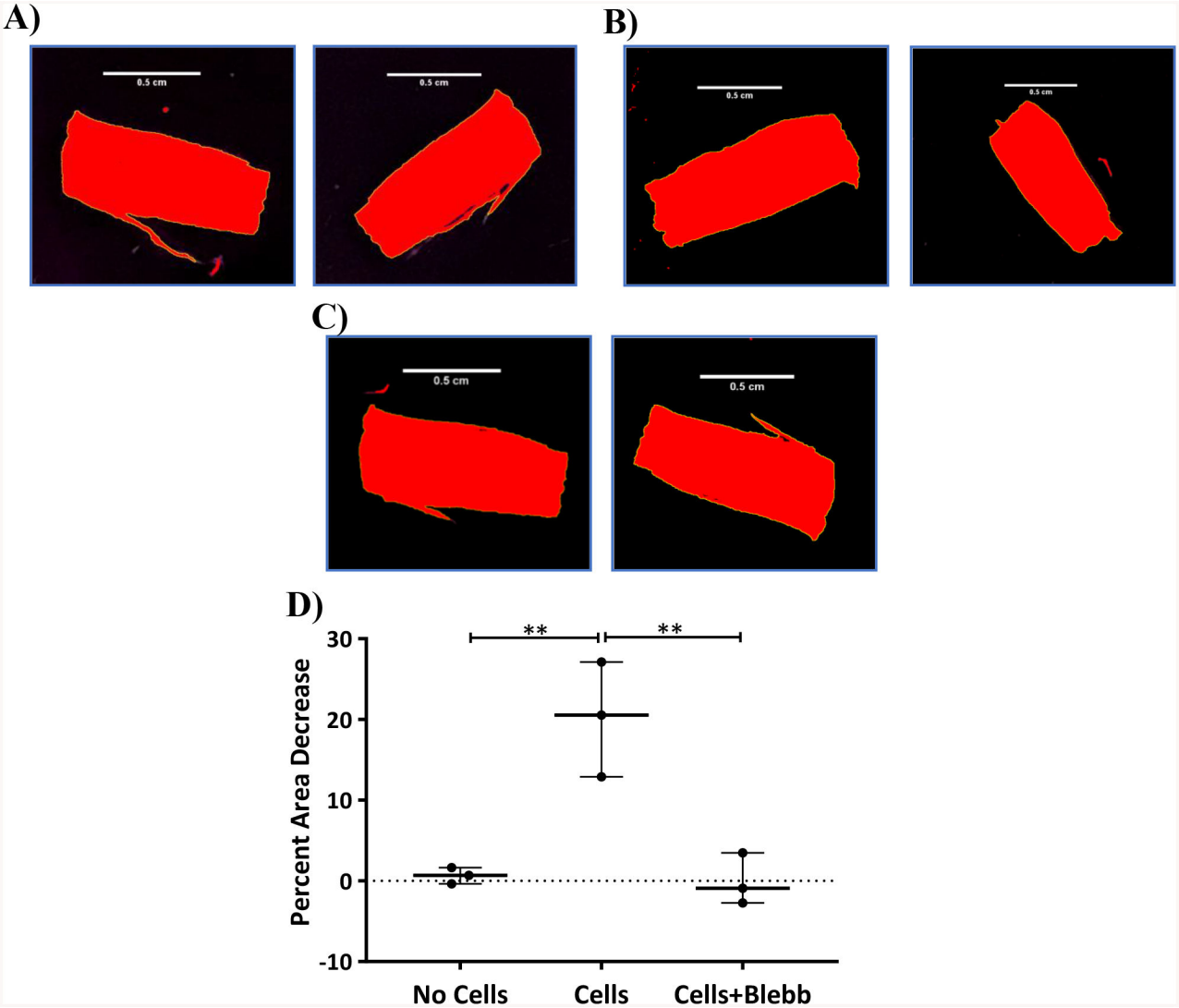

Figure 5:

Top – Brightfield images of DTS that were processed using ImageJ for threshold adjustment before (left) and after (right) 24 h of seeding cells. **A)** No cells **B)** Cell control **C)** 50 μM blebbistatin treatment. **Bottom – D)** Chart showing the percent area decrease of ECMs after 24 h with respect to various treatments. Statistical analysis was performed using a one-way ANOVA and Tukey post hoc test with n=3. *p<0.05; **p<0.01

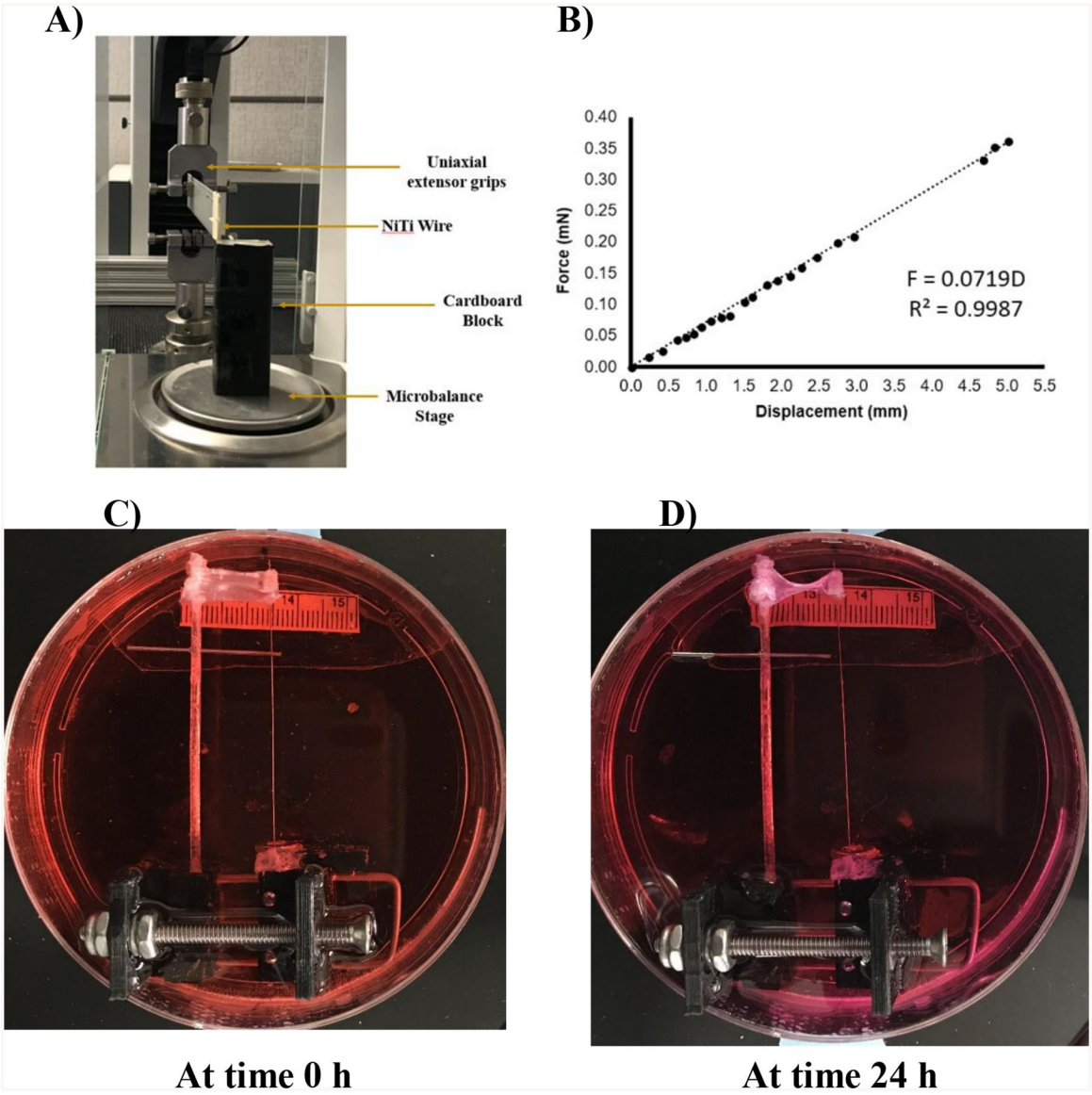

Figure 6:

Top A) Figure showing the process of calibration of a NiTi wire using a microbalance. **B)** Graph showing the calibration plot of NiTi wire via measurement of force with respect to displacement. **Bottom** figures showing the process of measuring force exerted by human TERT fibroblasts seeded on DTS and transferred onto the rigid rod/NiTi wire system after 6 h of seeding cells. **C)** At time 0 h after transferring cell seeded DTS. **D)** At time 24 h after transferring cell seeded DTS. Approximately 1 mm displacement in NiTi wire was observed equating to the force exertion of approx. 72 nN/30,000 cells or 2.4 pN per cell.

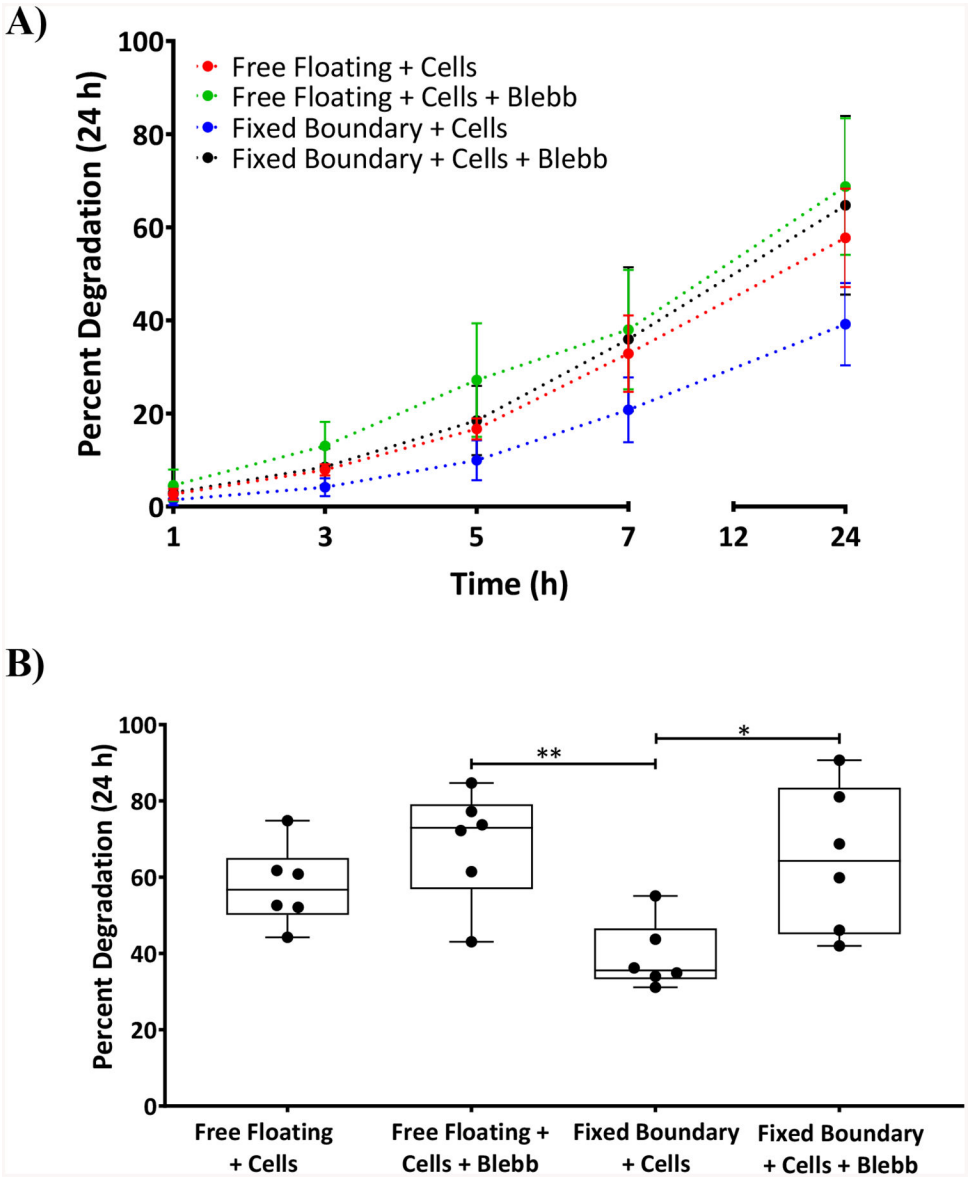

Figure 7:

A) Graph showing the percent degradation of ECMs after cell contractile force exertion with fixed boundary conditions and free floating in the presence and absence of blebbistatin at time points 1, 3, 5, 7, and 24 h. **B)** For the sake of clarity, the same 24 h data point as shown in Figure 7 A was represented in a bar graph showing the percent degradation of DTS that are subjected to free floating and fixed boundary conditions and treated or untreated with blebbistatin. Statistical analysis was performed using a one-way ANOVA and Tukey post hoc test with n=6. $*p<0.05$, $**p<0.01$

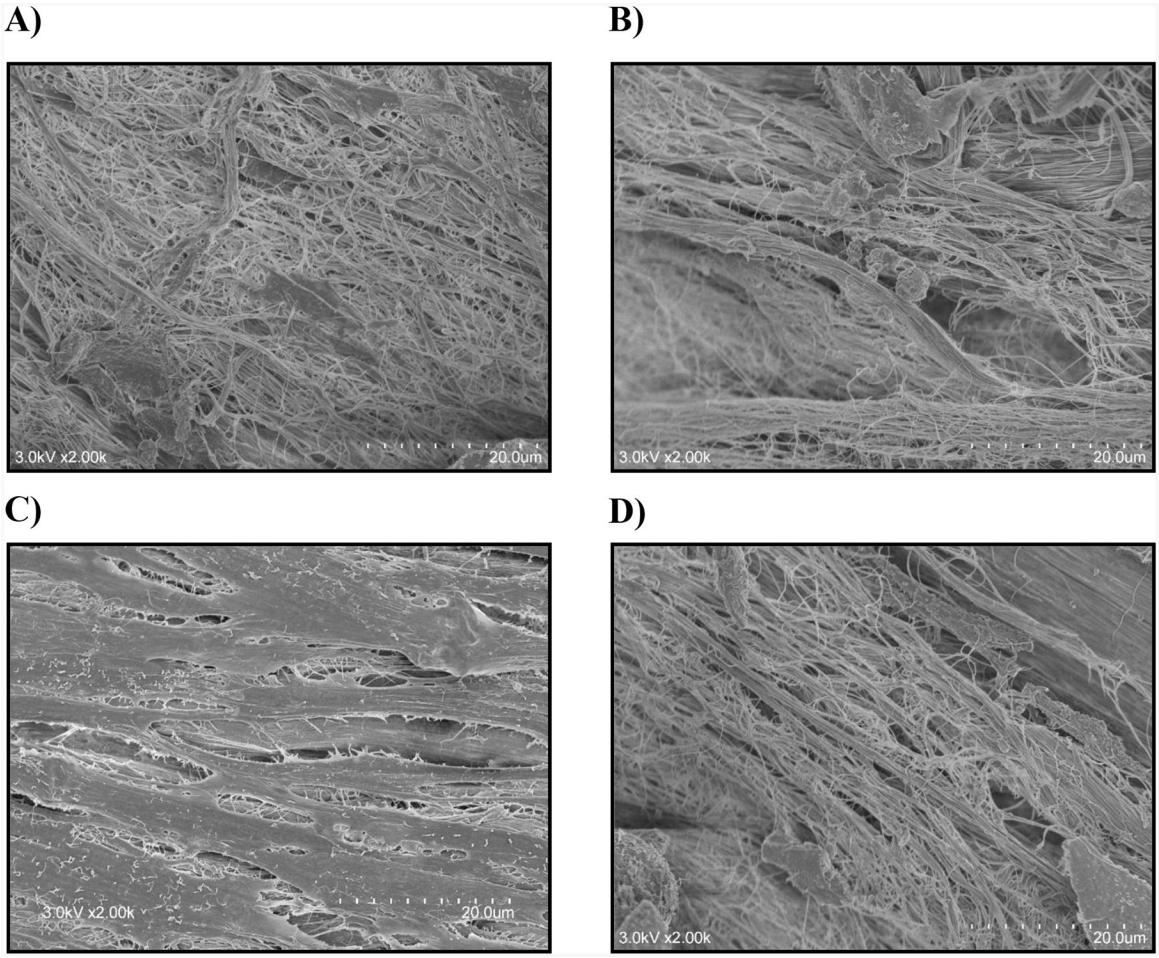

Figure 8:

Representative SEM images after 7 h of collagenase treatment of **A)** free floating DTS with cells; **B)** free floating DTS with cells and blebbistatin; **C)** DTS with cells and fixed boundaries; **D)** DTS with cells, treated with blebbistatin and with fixed boundaries